Current Biology 23, 1527–1535, August 19, 2013 ©2013 Elsevier Ltd All rights reserved http://dx.doi.org/10.1016/j.cub.2013.06.058

Article

Dauer-Specific Dendrite Arborization in *C. elegans* Is Regulated by KPC-1/Furin

Nathan E. Schroeder,[1] Rebecca J. Androwski,[1] Alina Rashid,[1] Harksun Lee,[2] Junho Lee,[2] and Maureen M. Barr[1,*]

[1]Department of Genetics and The Human Genetics Institute of New Jersey, Rutgers University, 145 Bevier Road, Piscataway, NJ 08854 USA

[2]Research Center for Functional Cellulomics, Institute of Molecular Biology and Genetics, Seoul National University School of Biological Sciences, Seoul 151-747, Republic of Korea

Summary

Background: Dendrites often display remarkably complex and diverse morphologies that are influenced by developmental and environmental cues. Neuroplasticity in response to adverse environmental conditions entails both hypertrophy and resorption of dendrites. How dendrites rapidly alter morphology in response to unfavorable environmental conditions is unclear. The nematode *Caenorhabditis elegans* enters into a stress-resistant dauer larval stage in response to an adverse environment.

Results: Here we show that the IL2 bipolar sensory neurons undergo dendrite arborization and axon remodeling during dauer development. When dauer larvae are returned to favorable environmental conditions, animals resume reproductive development and IL2 dendritic branches retract, leaving behind remnant branches in postdauer L4 and adult animals. The *C. elegans* furin homolog KPC-1 is required for dauer IL2 dendritic arborization and dauer-specific nictation behavior. KPC-1 is also necessary for dendritic arborization of PVD and FLP sensory neurons. In mammals, furin is essential, ubiquitously expressed, and associated with numerous pathologies, including neurodegenerative diseases. While broadly expressed in *C. elegans* neurons and epithelia, KPC-1 acts cell autonomously in IL2 neurons to regulate dauer-specific dendritic arborization and nictation.

Conclusions: Neuroplasticity of the *C. elegans* IL2 sensory neurons provides a paradigm to study stress-induced and reversible dendritic branching, and the role of environmental and developmental cues in this process. The newly discovered role of KPC-1 in dendrite morphogenesis provides insight into the function of proprotein convertases in nervous system development.

Introduction

Animals display numerous adaptations in response to stressful environmental conditions. Under ideal environmental conditions, the nematode *C. elegans* develops from an embryo through four larval stages before molting into the reproductive adult [1]. Under stressful conditions of high population density, starvation, and high temperature, *C. elegans* develops into an alternative larval stage called dauer (Figure S1 available online) [2]. Dauers are morphologically and behaviorally distinct from the nondauer third-larval L3 stage and adapted to survive stressful environmental conditions [3]. One adaptation is nictation behavior, mediated by the IL2 neurons, wherein the dauer larvae stand on their tail [3, 4]. Upon return to a favorable environment, dauers reenter reproductive development (Figure S1) [2, 5].

Differences in neuron morphology and gene expression are known to exist between dauers and nondauers [6–8]. However, the nervous system of dauers is relatively unexplored compared to the adult hermaphrodite. Electron microscopy studies found differences between *C. elegans* dauers and nondauers in the ciliated endings of neurons and surrounding glia [8, 9].

Most neurons in *C. elegans* are morphologically simple [10]. Electron microscopy and reconstruction of the *C. elegans* nervous system suggested that there were few, if any, branching dendrites [10]. However, recent studies using GFP revealed that the PVD and FLP polymodal sensory neurons undergo progressive dendritic arborization with increasing complexity as the animal develops from L2 to adult (reviewed in [11]).

Here we show that the IL2 neurons undergo dramatic remodeling during dauer development, including dendrite arborization. After an exit from dauer, IL2 processes retract and return to the nondauer morphology. Using a candidate-gene approach, we identified the POU homeodomain transcription factor UNC-86 and RFX transcription factor DAF-19 as regulators of dauer IL2 remodeling. From a forward genetic screen, we identified KPC-1, the *C. elegans* homolog of furin, as a cell-autonomous regulator of dauer-specific IL2 arborization and function.

Results

Dauer IL2 Neurons Display Dendrite Arborization and Multipolarity

In nondauer larvae and adults, the six IL2 neurons (left-right pairs located in the subdorsal, subventral, and lateral hexaradiate zones) have single unbranched primary (1°) dendrites, ending in sensory cilia that are exposed to the external environment (Figure 1A) [10, 12]. Although the six IL2 neurons have a similar gross structure during nondauer stages and express many of the same genes, the lateral IL2s display different neuronal connectivity and morphology [10, 12, 13]. Based on these observations and the anatomical differences described herein, we refer to the dorsal and ventral IL2 neurons as IL2Qs (inner labial type 2 quadrants), while the left and right IL2s are referred to as IL2Ls (inner labial type 2 laterals). This nomenclature is currently used for a set of six sensory outer labial neurons [10].

Using multiple fluorescent reporters expressed in the IL2s, we found that during dauer the IL2Qs undergo dendrite arborization resulting in a 3-fold increase in total dendritic length (Figures 1 and S2A). Remodeling of IL2 axons was also observed, including branching and axonal thickening (Figure S2B).

The IL2Q dendritic arbors in dauers are distinct and more variable in structure from the well-characterized and highly

*Correspondence: barr@dls.rutgers.edu

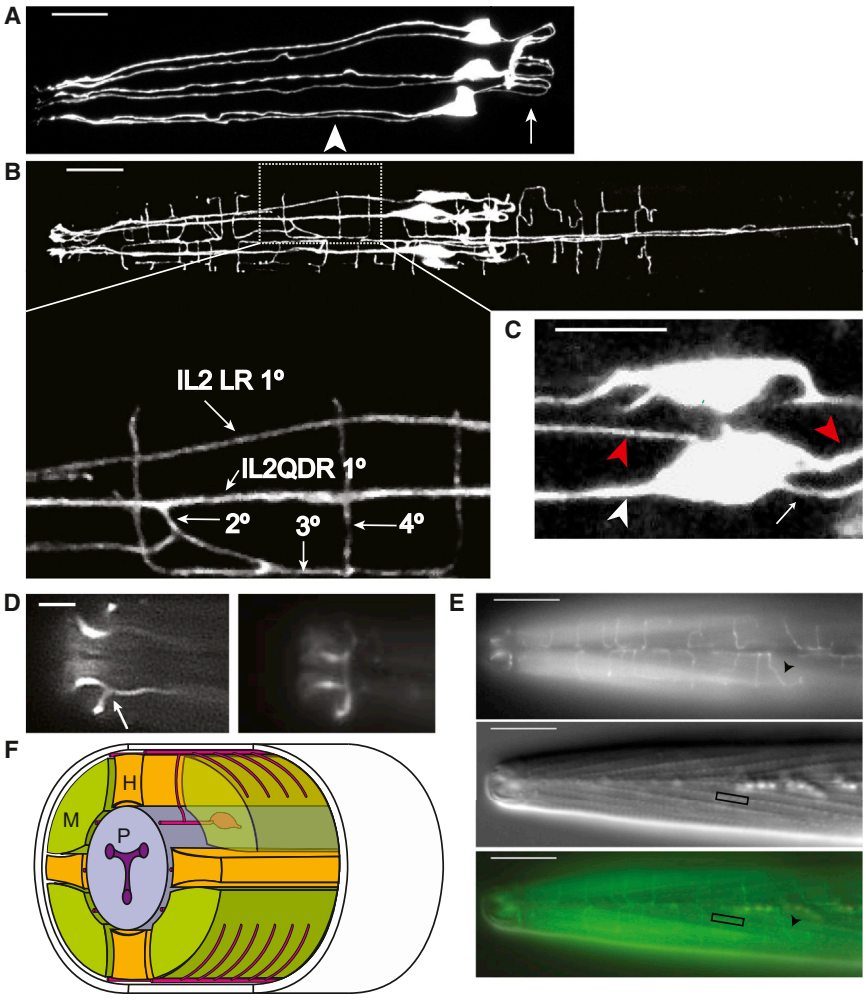

Figure 1. The IL2 Neurons Show Extensive Remodeling during Dauer

(A) Lateral z projection of a wild-type L3 expressing P_{klp-6}::GFP in IL2s. The six IL2s are arranged in a hexaradiate pattern with single 1° dendrites (arrowhead) anterior of the cell body. Axons (arrow) posterior from the cell body form a loop that innervates the nerve ring. The scale bar represents 10 μm.

(B) Dorsal z projection of wild-type dauer expressing P_{klp-6}::GFP in IL2s. The IL2Q (for quadrant) dendrites in dauer are highly branched. Zoomed inset: the IL2QDR 1° dendrite extends a 2° dendrite toward the dorsal midline which branches, forming a 3° dendrite that travels along the dorsal midline. This 3° dendrite branches and extends 4° dendrites into the body-wall muscle quadrants. Similar branching patterns are seen on the ventral body wall. The scale bar represents 10 μm.

(C) z projection of IL2QDL dauer cell body expressing P_{klp-6}::GFP. The IL2Qs extend additional dauer-specific primary dendrites (1d°) (red arrowheads) in addition to the original nondauer anteriorly directed 1° dendrite (white arrowhead), and posteriorly directed axon (white arrow). The scale bar represents 5 μm.

(D) Dorsal view of dauer nose expressing P_{lag-2}::GFP showing (left) the single branch (arrow) extending from the lateral IL2LL 1° dendrite and (right) a body-wall view of the same animal showing the formation of the crown from branches emerging from the IL2L dendrites. The scale bar represents 5 μm.

(E) Wild-type dauers extend fine dendritic processes along the body wall. Top: dorsal/ventral view of body wall in a wild-type dauer expressing P_{lag-2}::GFP in IL2 neurons. Quaternary dendrites (arrowhead) extend from the dorsal/ventral midlines perpendicularly into the muscle quadrants. Middle: same animal and focal plane with DIC Nomarski optics. Somatic muscle dense bodies (box), which serve as connections with the overlying hypodermis, are evident. Bottom: merged image. Scale bars represent 10 μm.

(F) Oblique transverse schematic of dauer IL2 branching. M, muscle; P, pharynx; H, hypodermis.

See also Figure S2.

stereotyped PVD dendritic arbors in adults [14]. During dauer, the IL2Q 1° dendrites extend secondary (2°) dendrites directly to the dorsal (for IL2QDs) and ventral (for IL2QVs) midlines (Figures 1B and 1F). This differs from PVD neurons where the 2° dendrites travel along the body wall dorsally and ventrally to the sublateral nerves (see Figure 2A in [14]). Upon reaching the dorsal or ventral midline, the IL2Q 2° dendrites branch and extend 3° dendrites in anterior and posterior directions along the midlines. As the IL2Q 3° dendrites travel along the midline, they extend 4° dendrites perpendicular from the midline into the body-wall muscle quadrants (Figures 1B and 1F). Each 4° dendrite is spaced and does not overlap with another, suggestive of self-avoidance. Occasionally, a given 4° dendrite branches again, producing a 5° dendrite that extends the potential receptive field in the body wall. Generally, the body-wall 4° dendrites will remain in the ipsilateral body-wall quadrant. In rare instances, we observed wild-type (WT) dauers whose dendrites crossed the dorsal or ventral midlines and extended 4° dendrites to the contralateral side (Figure S2C).

In addition to dendritic branches emerging from the 1° dendrites, dauer IL2Qs extend additional 1° dendrites from the cell bodies, resulting in a shift from bipolar to multipolar neurons. We refer to these additional dendrites as dauer-specific primary (1d°) dendrites (Figure 1C). The 1d° dendrites extend to both the dorsal/ventral midlines as well as the lateral midlines and remain within the ipsilateral body quadrant. For example, the IL2QDL may send 1d° dendrites to both the dorsal and lateral left midlines. Upon reaching the midlines, the 1d° dendrites branch to form 2d° dendrites that extend in anterior and posterior directions. The 2d° dendrites then branch and extend 3d° dendrites perpendicular into the ipsilateral body-wall field, similar to the 4° dendrites that originate from the 1° dendrites.

The IL2Ls remodel during dauer in a pattern distinct from the IL2Qs. The dauer IL2Ls extend only a single 2° dendrite, at the distal end of the 1° dendrite, toward the lateral midline. Upon reaching the midline, the IL2L 2° dendrite extends 3° dendrites around the circumference of nose. Frequently (~50% in WT), the 3° dendrites from each lateral IL2 neuron meet to form a crown-like structure (Figure 1D). It is uncertain whether the crown processes fuse as seen with the amphid sheath cells in dauers [8, 9].

After a return to favorable environmental conditions, dauers recover and reenter reproductive developmental [2]

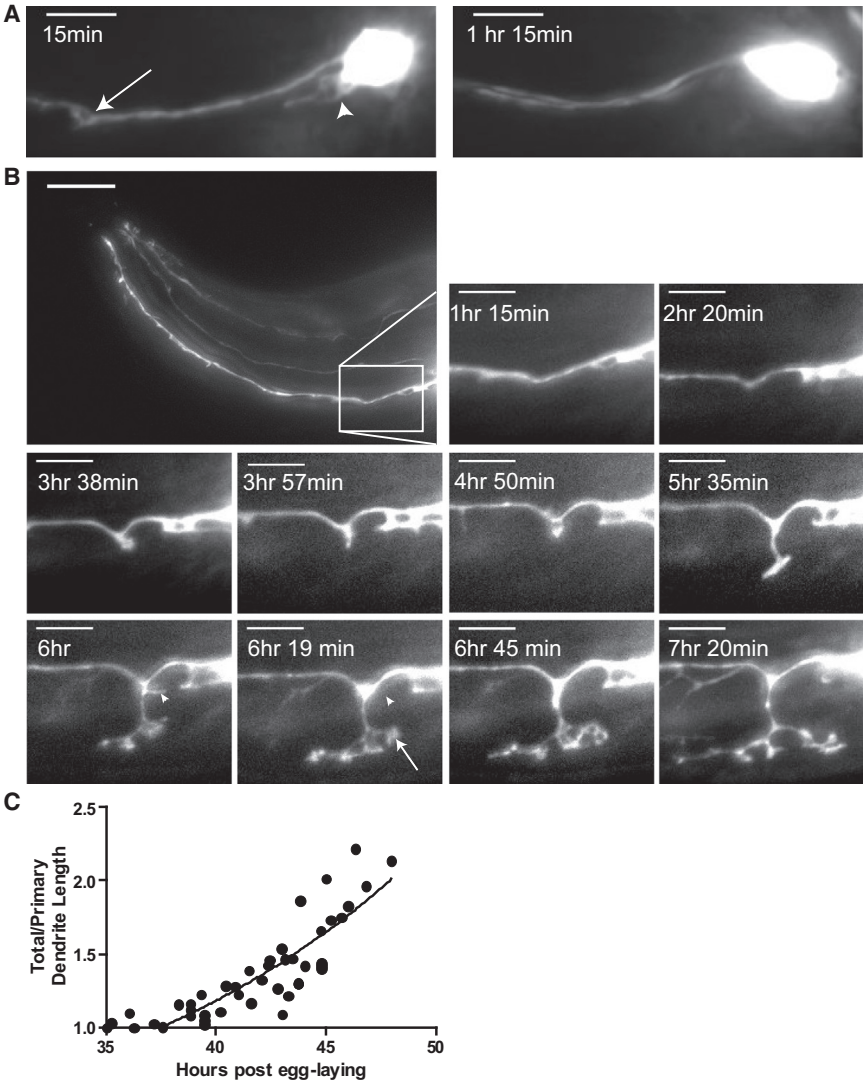

Figure 2. Time-Lapse Imaging of IL2Qs during Dauer Formation Reveals Rapid Dendrite Arborization

(A) z projection time-lapse images of a single animal expressing P_{klp-6}::tdTomato after the onset of the L2d molt into dauer. Fifteen minutes after the L2d molt, 2° dendritic sprouts (arrow) and 1d° dendrites (arrowhead) appear on an IL2QDL neuron. Seventy-five minutes after the onset of the L2d molt, these sprouts have retracted. The scale bar represents 10 μm.

(B) Lateral z projection time-lapse images of single animal expressing P_{klp-6}::tdTomato during the L2d molt into dauer. The formation of putative growth cones (arrow at 6 hr 19 min) as well as the retraction of branches (arrowheads at 6 hr and 6 hr 19 min) of IL2Qs is seen. Inset scale bars represent 5 μm.

(C) Quantification of relative IL2Q dendritic length during dauer formation after the onset of the L2d molt fits an exponential curve [$Y = 0.849*e^{(0.066x)}$, $R^2 = 0.7436$]. A ratio of total/primary dendritic length was used to adjust for changes in total body length. Each animal examined is represented by multiple time points (n = 9 animals, 5–25 time points per animal).

(Figure S1). During the 12–15 hr recovery period, the IL2 dendritic arbors retract, leaving behind remnant branches. Remnant branches, typically short 2° or 1d° dendrites that approach but rarely meet the midline, are seen in 75.6% (n = 41) of postdauer L4 and adult animals (Figure 3A). This result illustrates the influence of the environment and early developmental events on the adult nervous system.

IL2 dendritic arborization is observed in 100% of wild-type dauers from starved conditions or induced through exposure to dauer pheromone. Mutations in *daf-2* and *daf-7*, which cause constitutive dauer formation under favorable environmental conditions, also result in dauer-specific IL2 arborization. Exposure to dauer-inducing conditions in nondauer animals does not result in IL2 arborization (data not shown). We do not observe similar arborization during dauer in the following neurons: touch receptor neurons, PVDs, FLPs, CEPs, amphid, and phasmid neurons. Together, these data suggest that the IL2s possess the ability to dynamically remodel and that arborization is an inherent component of the many morphological and behavioral adaptations seen during dauer.

Development of Dauer-Specific IL2Q Morphology Is a Rapid and Dynamic Process

To follow the development of dauer-specific IL2Q arborization, we performed time-lapse imaging of the IL2Qs during the molt into dauer (Figure S1). At the beginning of this molt, an initial 1d° dendrite forms on the IL2Q cell bodies (Figure 2A) and retracts soon after the closure of the stoma. After the original 1d° extension and retraction event, short puncta form and retract along the length of the original 1° dendrite over the next 3-4 hr (Figure 2B). Approximately 5–6 hr after molt onset, coinciding with the shrinking of the pharynx, several of the 2° dendritic sprouts extend toward the ventral or dorsal midlines. Approximately 6–8 hr after molt onset, the developing 2° dendrites rapidly grow in an exponential fashion, forming growth cones and 3° dendrites that expand and collapse (Figure 2B, compare 6 hr to 6 hr 19 min). Once the 2° dendrites reach the dorsal and ventral midline, they branch to form both anteriorly and posteriorly directed 3° dendrites. Continued observation beyond approximately 8 hr after molt onset was technically impossible due to radial shrinkage and subsequent movement within old cuticles. In summary, dendritic arborization begins slowly and rapidly increases, leading to an exponential increase in total dendritic length (Figure 2C).

We examined the morphology of IL2 neurons after a transfer of dauers to favorable environmental conditions (plentiful food, low population density) (Figure 3). While commitment to dauer recovery is made within the first hour upon return to favorable conditions [5], no obvious changes in IL2 arbors are seen in dauers during the first hour after transfer. Within 3 hr in favorable conditions, loss of the 4° body-wall dendrites first occurs. Almost all 4° body-wall dendrites are retracted by

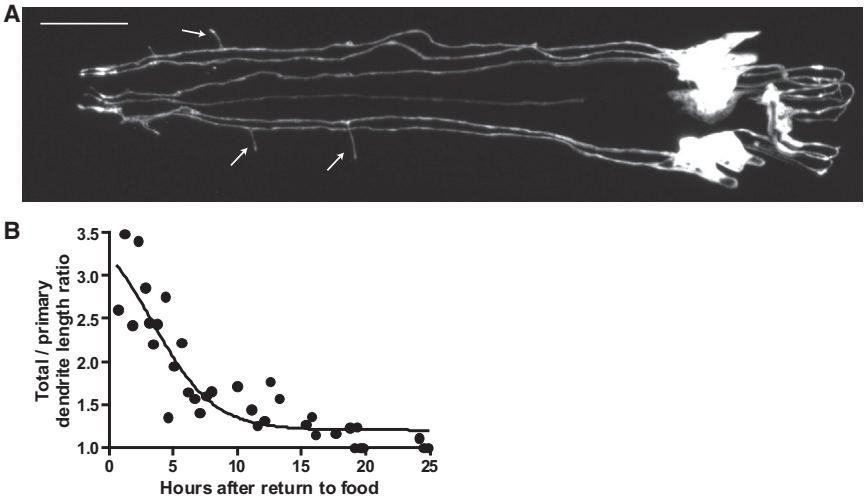

Figure 3. After Recovery from the Dauer Stage, IL2Q Arbors Undergo Incomplete Retraction

(A) Lateral z projection of a postdauer L4 expressing P_{klp-6}::GFP. Nematodes often will retain short remnant 2° (arrows) dendrites following recovery from dauer. The scale bar represents 10 μm.

(B) Quantification of relative IL2Q dendrite length after the return of dauers to favorable conditions (plentiful food, low population density) fits a sigmoidal response curve [$Y = 1.24 + (2.518 \div [1+10^{(0.183x - 0.616)}])$, $R^2 = 0.803$]. A ratio of total/primary dendritic length was used to adjust for changes in total body length. Each data point represents a separate animal (n = 35 animals).

the onset of pharyngeal pumping (3–4 hr after transfer to food); however, 2° dendrites and 1d° dendrites are still present. Most branches are retracted, albeit often incompletely, at the molt into L4 (12–14 hr after transfer) (Figure 3).

IL2Q and IL2L Dendritic Morphology Are Regulated by Independent Transcription Factors

To begin to understand the mechanisms regulating dauer-specific IL2 branching, we examined several candidate genes. The POU homeodomain transcription factor UNC-86 is required for cell identity of several neurons, including PVD and IL2 [15]. UNC-86 also controls dendritic outgrowth in PVD [16]. As expected, null alleles of *unc-86* result in a complete lack of IL2 reporter GFP expression, presumably due to cell-fate defects (data not shown). However, the *unc-86(n848)* reduction-of-function mutant [17] possesses IL2 neurons with normal cell somas, axons, and 1° dendrites. Additionally, *unc-86(n848)* mutants show normal expression of several IL2-specific reporters, suggesting retention of IL2 cell fate. Sequencing of *unc-86(n848)* revealed a point mutation at a splice donor site within the DNA-binding homeodomain (Figure S3C). Interestingly, *unc-86(n848)* causes a significant decrease in the number of 4° body-wall dendrites, resulting in a total decrease in dendritic length, number of branch points, and a redistribution of the arbor (Figures 4A, 4B, S3A, and S3B). These results indicate that *unc-86* is required for IL2Q dendritic arborization.

The helix-loop-helix transcription factor, LIN-32, acts in parallel with UNC-86 to determine IL2 cell identity [18]. Indeed, a hypomorphic *lin-32* mutant fails to express P_{klp-6}:: GFP in the full complement of six IL2 neurons ($\bar{x} = 1.71 \pm 0.97$ neurons/animal, n = 34 animals). However, typical dauer arborization is seen in IL2Q neurons that express P_{klp-6}::GFP (Figures 4B and S3D). The LIM homeodomain transcription factor MEC-3 is also required for PVD dendritic branching and acts in concert with UNC-86 for PVD and touch receptor neuron development [19, 20]. In *mec-3* mutants, IL2 dauer-specific arborization appears to be normal (data not shown).

The RFX transcription factor DAF-19 is a master regulator of ciliogenesis, with *daf-19(m86)* null mutants lacking all cilia [21, 22]. Interestingly, IL2Q branching is normal in *daf-19(m86)* mutants, suggesting that external signals sensed by the IL2Q cilia do not directly initiate IL2Q branching (Figure 4B). In WT dauers, the IL2Ls extend only a single 2° process that forms a crown-like structure (Figure 1D). However, *daf-19(m86)* dauers often display an additional 2° processes on one or both IL2Ls [19/34 *daf-19(m86)* with extra IL2L processes, 1/21 WT with extra IL2L processes, $p < 0.001$, Fisher's exact test] (Figure 4C). We next examined the IL2s in *daf-19(n4132)*, an allele that disrupts a DAF-19 isoform necessary for the function but not development of IL2 cilia [13]. Interestingly, *daf-19(n4132)* dauers do not display additional IL2L processes (n = 24 animals). These results indicate that either DAF-19 is acting outside of the IL2Ls to inhibit additional processes in dauers or that the presence of IL2 cilia has an inhibitory action on IL2L process formation. Combined, these data are consistent with the IL2Qs and IL2Ls being two separate neuronal classes.

KPC-1, a Furin Proprotein Convertase Homolog, Is Necessary for Proper Dendrite Arbor Organization

To identify novel genes involved in dauer-specific branching, we performed a mutagenesis screen. We examined approximately 1,500 haploid genomes for mutants with defects in dauer-specific IL2 remodeling. From this screen, we isolated an allele of the proprotein convertase (PC)-encoding gene, *kpc-1* (*K*ex2/*p*roprotein *c*onvertase). *kpc-1(my24)* mutants have highly disorganized and truncated dauer-specific IL2Q branching with 100% penetrance (Figure 5A and the Supplemental Experimental Procedures). *kpc-1(my24)* dauers show resistance to 1% SDS and no obvious defects in dauer formation or recovery or in IL2 retraction after dauer recovery. Non-dauer *kpc-1* mutants show no obvious defects in dendrite morphology (Figure S5A).

PCs are highly conserved serine proteases that cleave numerous proproteins into their active forms [23]. PCs contain an N-terminal signal peptide and prodomain that is autocatalytically cleaved (Figure 5B). The catalytic domain contains conserved aspartate, histidine, and serine residues that serve as the catalytic triad necessary for nucleophilic attack of cleavage sites [24]. The conserved "P domain" is essential for PC function and is thought to stabilize the PC [25]. The C terminus is variable among PCs and may include transmembrane and cysteine-rich domains [24, 26].

kpc-1(my24) introduces a missense mutation resulting in a P440L amino acid change at a highly conserved proline four residues C-terminal to the catalytic serine (Figure 5B). Examination of the crystal structure of mouse furin [27] shows that the homologous proline is located within the catalytic pocket and a change to a leucine residue may obstruct cleavage of

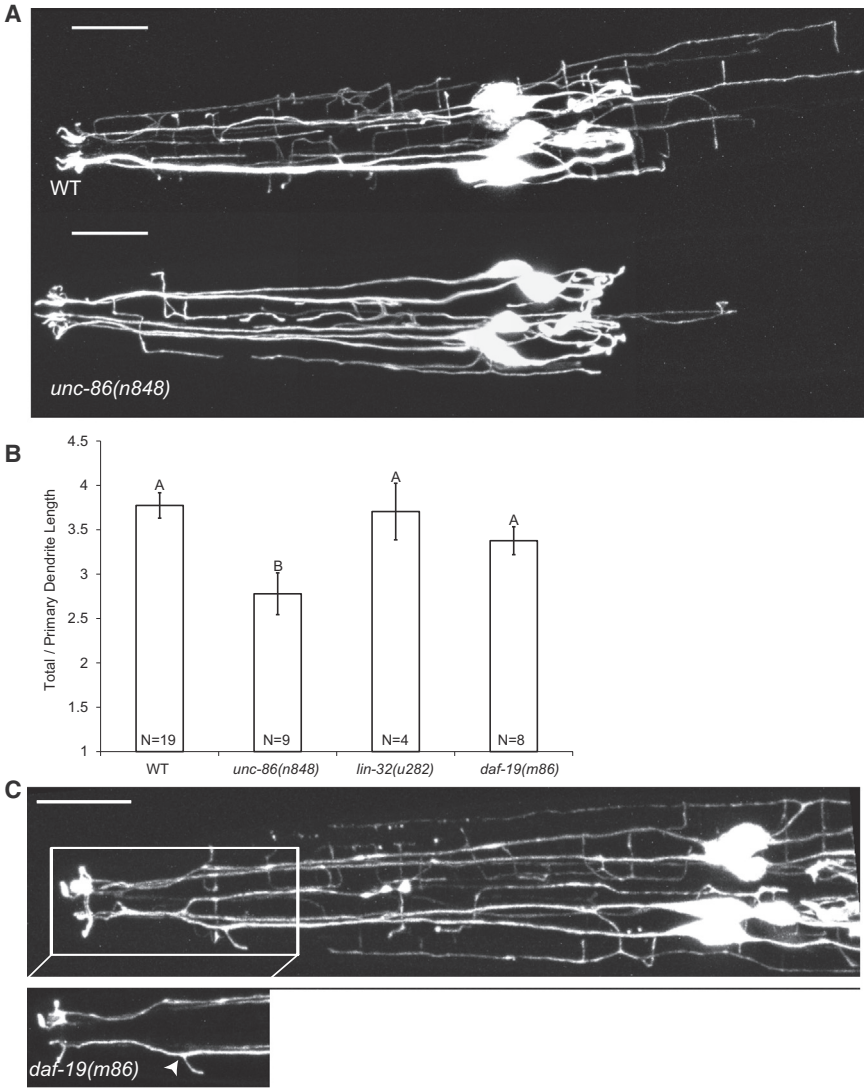

Figure 4. The Transcription Factors UNC-86 and DAF-19 Regulate Distinct Components of Dauer-Specific IL2 Remodeling

(A) z projections of WT (top) and *unc-86(n848)* (bottom) dauers expressing $P_{F28A12.3}$::GFP. Scale bars represent 10 μm.

(B) *unc-86(n848)* dauers show significantly smaller IL2Q arbors than the WT. Dendritic length was measured as a ratio of total/primary dendritic length to compensate for differences in body length between genotypes. Data are mean ± SEM. Genotypes with different letters above bars are statistically different ($\alpha = 0.01$) as determined by ANOVA followed by Tukey's post hoc test for comparison of multiple genotypes.

(C) Dorsal z projection of *daf-19(m86)* dauer expressing $P_{F28A12.3}$::GFP with inset of IL2LL dendrite showing supernumerary branching (arrowhead). The scale bar represents 10 μm.

See also Figure S3.

substrates (Figure S4). *kpc-1(my24)* fails to complement *kpc-1(gk8)*, a previously isolated deletion allele that removes most of the catalytic domain (Figure 5B). Furthermore, *kpc-1(my24)* and *kpc-1(gk8)* display a similar severity of IL2 branching defects, suggesting that *kpc-1(my24)* is a loss-of-function allele (Figure S5B). There are four PCs encoded in the *C. elegans* genome [28]. However, mutations in the other three PC genes, *bli-4*, *aex-5*, and *egl-3*, do not produce obvious defects in IL2 dauer-specific dendritic branching, indicating a unique role for KPC-1 among the PCs in IL2 remodeling during dauer (data not shown).

We next explored the role of KPC-1 in the multidendritic sensory neurons PVD and FLP. We found that, similar to the IL2 dauer arbors, the PVD and FLP multidendritic arbors are highly disorganized and truncated in adult *kpc-1* mutants (Figures 5C and S5C). Interestingly, previous microarray data identified *kpc-1* as upregulated in the PVDs during arborization [16]. *kpc-1* mutants are wild-type for amphid, phasmid, and IL2 dye filling and showed no obvious defects in touch-receptor neuron morphology (data not shown) or function [29]. These data suggest that KPC-1 is necessary for proper organization of multidendritic arbors in *C. elegans.*

KPC-1 Acts Cell Autonomously to Regulate Dauer-Specific IL2 Arborization

Using a transcriptional reporter consisting of the 3 kb 5′ region upstream of *kpc-1* fused to GFP (P_{kpc-1}::GFP), we found that *kpc-1* is expressed in numerous neuronal and epithelial cells during dauer (Figure 6A). Processes adjacent to the body wall in dauers resemble those of IL2Q 4° dendrites (Figure 6B). To determine whether *kpc-1* is expressed in the IL2s, we coinjected the P_{kpc-1}::GFP reporter with a P_{klp-6}::tdTomato reporter that is expressed exclusively in the IL2s. During nondauer stages, *kpc-1* is not expressed in the IL2 neurons (data not shown). In dauers, P_{kpc-1}::GFP and P_{klp-6}::tdTomato are coexpressed, indicating that *kpc-1* is upregulated in the IL2s during dauer (Figure 6C). Nondauer expression was consistently observed in the ventral nerve cord and pharynx with strong expression in the g2 pharyngeal gland cells and vpi pharyngeal intestinal valve cells (Figures S6).

We next asked whether KPC-1 acts cell autonomously in the IL2s to control dauer-specific branching. We expressed KPC-1(+) under the control of the IL2-specific *klp-6* promoter (P_{klp-6}::KPC-1) in a *kpc-1(gk8)* mutant background. The P_{klp-6}::KPC-1 transgene is sufficient to rescue the *kpc-1* IL2 branching phenotype, indicating that KPC-1 acts cell autonomously to control dauer-specific IL2 arborization (Figure 6D).

To determine the subcellular localization of KPC-1, we created a translational reporter consisting of the 3 kb 5′ region and the entire *kpc-1* genomic sequence fused to dsRed. KPC-1::dsRed rescues the *kpc-1(gk8)* branching phenotype, indicating that the transgene is functional in IL2 neurons (Figure 6D). The KPC-1 subcellular localization differs among neuronal types. In the majority of neurons, including the IL2s, KPC-1::dsRed is nonnuclear and excluded from all but the most proximal segments of the 1° dendrite and axon (Figure 6E). In ventral cord neurons, KPC-1 localizes to cell bodies and processes (Figure S6B).

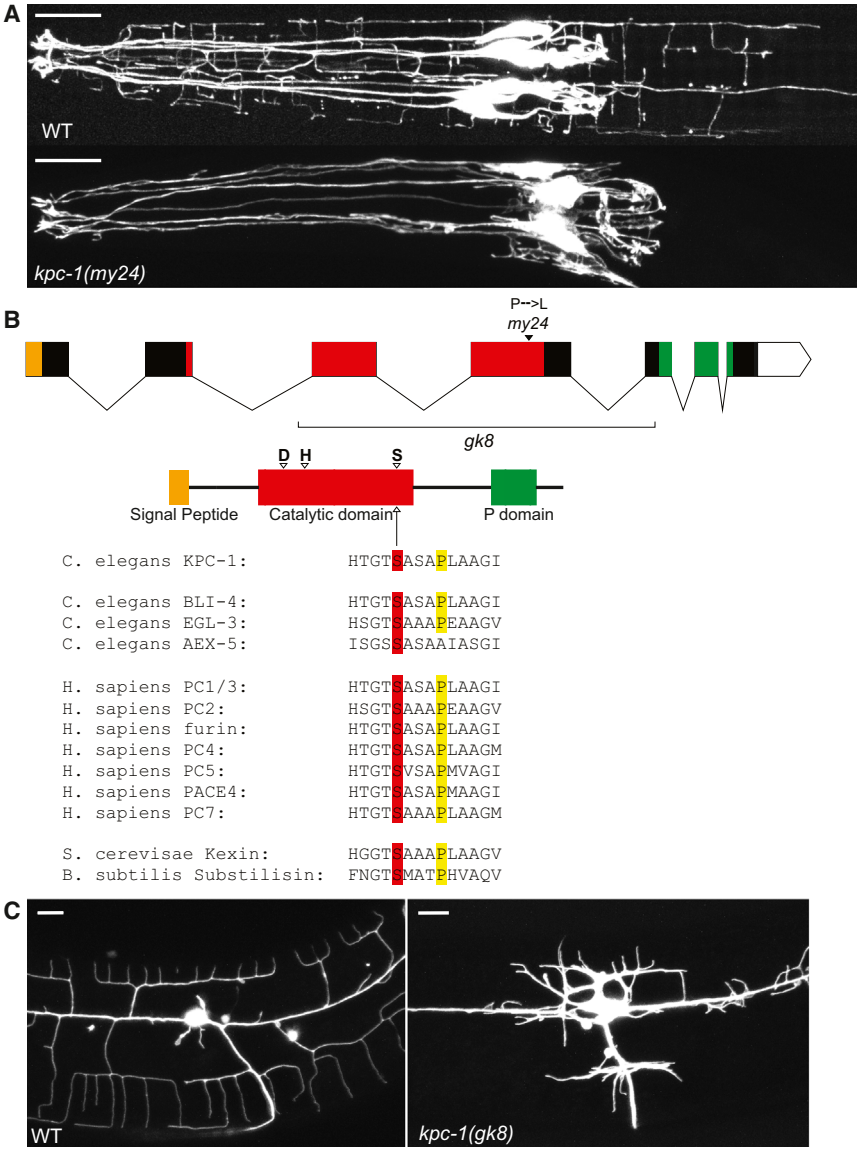

Figure 5. KPC-1 Is Required for Multidendritic Neuron Arborization

(A) z projections of wild-type (top) and *kpc-1(my24)* (bottom) dauers expressing P_{klp-6}::GFP. Disruption of *kpc-1* results in disorganized IL2 dendritic arbors in 100% of animals examined (n > 100). See also Figure S5. The scale bar represents 10 μm.

(B) Exon/intron diagram of *kpc-1*. The *kpc-1(my24)* allele introduces a c→t missense mutation resulting in a P440L amino acid change at a highly conserved residue (highlighted yellow in alignment) four amino acids C-terminal from the catalytic serine (highlighted red in alignment). The *kpc-1(gk8)* deletion allele removes the majority of the catalytic domain.

(C) Lateral z projections of PVD neurons in wild-type (left) and *kpc-1(gk8)* (right) adults expressing $P_{F49H12.4}$::GFP. Similar to the IL2 neurons, disruption of *kpc-1* leads to disorganized and truncated arbors in PVDs. See also Figure S5C. The scale bar represents 10 μm.

See also Figures S4 and S5.

KPC-1 Regulates Movement in Both Dauers and Nondauers

The *kpc-1(gk8)* is described as having a slight uncoordinated phenotype [28]. We find that adult *kpc-1* mutants show fewer body bends than do WT animals (Figure S6C). Adult motility is not rescued by the IL2-specific P_{klp-6}::KPC-1 transgene (data not shown). As *kpc-1* is expressed in the ventral nerve cord (Figure S6B), which regulates movement, it seems likely that *kpc-1* affects the function of these neurons.

Unlike nondauer larval and adult stages, dauers tend to remain motionless [2]. Dauers are uniquely capable of performing a behavior termed nictation in which the animal elevates the majority of its body into the air for extended periods of time [3]. In nature, this behavior is thought to facilitate transport of dauers to new nutrient rich environments by passing arthropods. The IL2 neurons are required for nictation in dauers [4]. We found that *kpc-1* and *unc-86(n848)* dauers are defective in nictation (Figure 7). As both *unc-86* and *kpc-1* mutants display motility defects, one possibility is that simply being uncoordinated (Unc) results in nictation defects. We previously examined the nictation behavior of several Unc or neurotransmitter/neuropeptide mutants, including the proprotein convertase mutant *egl-3* and GABA mutants *unc-26* and *unc-29*, and showed that these mutants are capable of nictation [4]. To determine whether *kpc-1* acts cell autonomously to regulate nictation, we expressed the IL2-specific P_{klp-6}::KPC-1 transgene in dauers and observed rescue of nictation defects. We conclude that *kpc-1* acts cell autonomously in IL2 neurons to regulate dauer-specific nictation behavior (Figure 7) and dendritic arborization (Figure 6D).

Discussion

Our finding of rapid and reversible dendritic arborization during dauer presents a new system for studying the molecular pathways leading from environmental stress to neuronal remodeling. Neuron morphology is affected by developmental and environmental conditions, and the dendritic processes of neurons appear to be acutely sensitive to changing environments [30]. For example, after exposure to stress, the mammalian brain undergoes contrasting patterns of dendrite resorption in the hippocampus and increased dendrite arborization in the amygdala [31]. In humans, alterations seen in dendrite morphology after extreme stress may serve a causative role in anxiety-related pathologies such as posttraumatic stress disorder [32].

Shared and distinct transcriptional mechanisms regulate PVD, FLP, and IL2Q arborization. For example, the POU homeodomain transcription factor UNC-86 regulates arborization in both PVD neurons [16] and IL2Q dauer neurons (Figures 4A and 4B), while the LIM homeodomain transcription factor MEC-3 acts in concert with UNC-86 to regulate PVD dendritic branching, but not IL2Q arborization. Our study does not directly separate developmental morphogenesis from stress-induced plasticity per se. As both *unc-86* and *kpc-1* are necessary for both PVD and dauer-specific arborization, it is likely

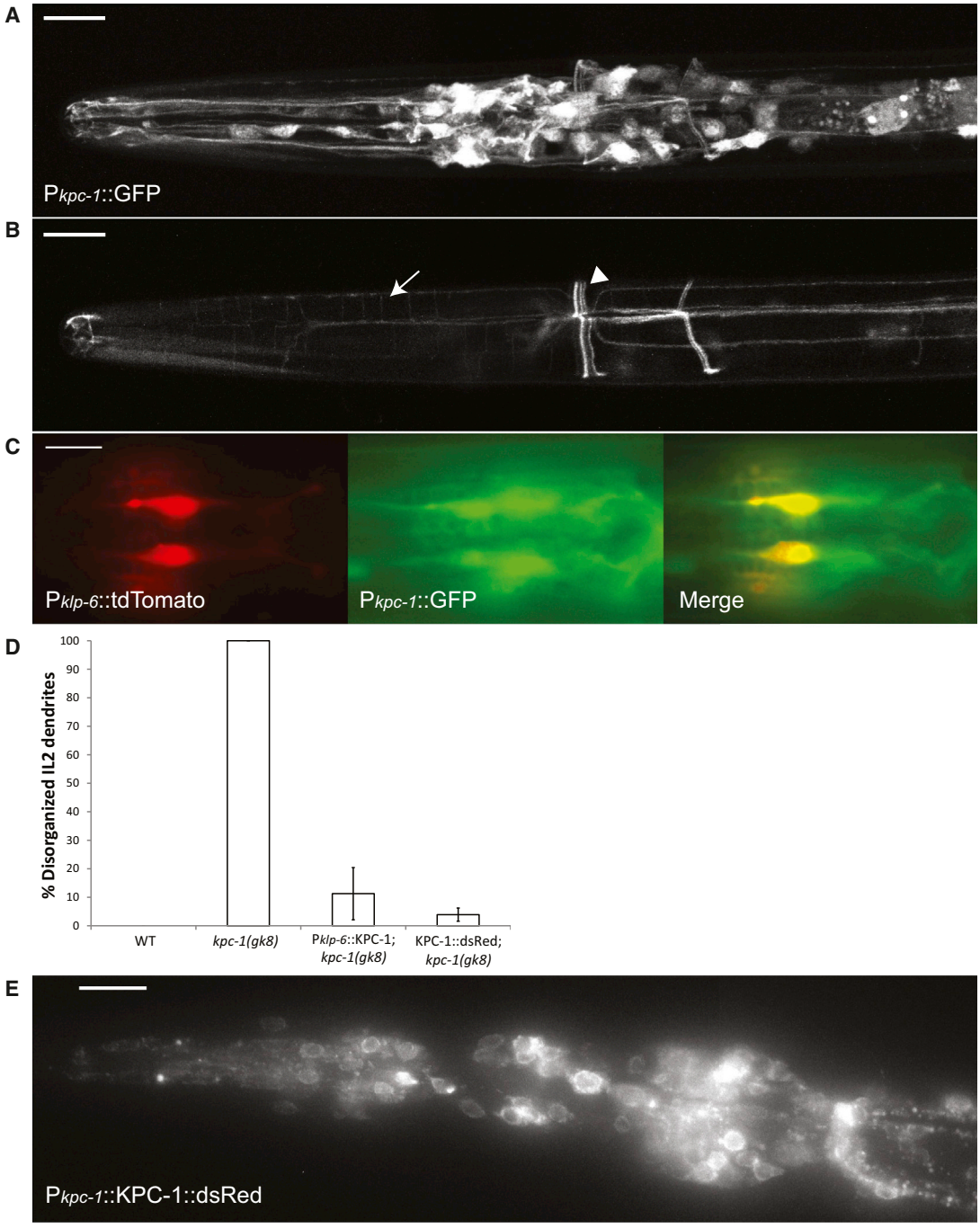

Figure 6. *kpc-1* Is Expressed Broadly but Acts Cell Autonomously to Regulate IL2Q Dauer-Specific Remodeling

(A) Ventral z projection of dauer expressing P_{kpc-1}::GFP with expression in numerous neuronal and nonneuronal cells throughout the head. The scale bar represents 10 μm.

(B) Ventral body-wall plane of same animal as in (A) showing GFP expression in IL2Q dauer-specific branches (arrow) as well as several additional neuronal commissures (arrowhead, amphid commisure). The scale bar represents 10 μm.

(C) Dauer expressing both the IL2-specific reporter P_{klp-6}::tdTomato (left) and P_{kpc-1}::GFP (middle). An overlay image (right) demonstrates that P_{kpc-1}::GFP is expressed in the IL2s. The scale bar represents 5 μm.

(D) *kpc-1(gk8)* defects in dauer-specific IL2Q arborization are rescued by constructs of either an IL2-specific promoter driving full-length wild-type *kpc-1* (P_{klp-6}::KPC-1) or full-length *kpc-1* tagged with dsRed and driven by the *kpc-1* endogenous promoter (KPC-1::dsRed). Rescue was assessed by examination of dauer-specific IL2Q arborization in *kpc-1(gk8)* dauers expressing P_{klp-6}::GFP in three independent transgenic lines (n = 22–25 dauers per line). A mean ± SEM of the three lines is given. Statistical tests comparing the rescued lines with the WT and *kpc-1(gk8)* cannot be performed due to a lack of variation in controls; however, P_{klp-6}::KPC-1 and KPC-1::dsRed are not statistically different (Fisher's exact test, p = 0.9303).

(E) z projection of *kpc-1(gk8)* dauer head expressing KPC-1::dsRed. In most neurons, KPC-1::dsRed is localized exclusively within the cell bodies and is not observed in neuronal processes. However, in the ventral nerve cord KPC-1::dsRed is found in both cell bodies and neuronal processes (see Figure S6B). The scale bar represents 10 μm.

See also Figure S6.

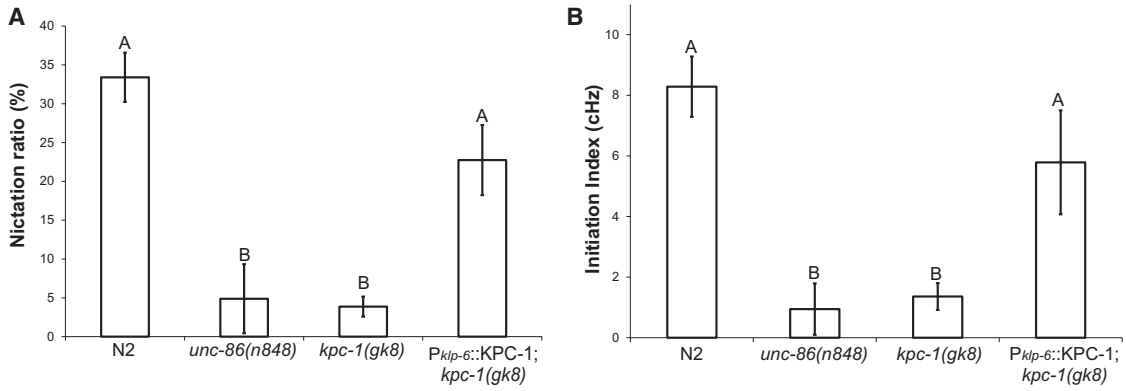

Figure 7. *kpc-1* and *unc-86* Regulate Nictation Behavior

(A) Quantification of percent time spent nictating versus nonnictating [(T_{nic} / T) × 100] in actively moving dauers as previously described [4]. *kpc-1* and *unc-86(n848)* mutant dauers are defective in nictation ratio, while IL2-specific rescue of *kpc-1* restores nictation ratio to WT levels.

(B) Quantification of nictation initiation index [N / (T_{nic} – T) × 100] as previously described [4]. *kpc-1* and *unc-86(n848)* mutants are defective, while IL2-specific rescue of *kpc-1* restores initiation index to WT levels.

Data are means ± SEM. Genotypes with different letters above bars are statistically different (α = 0.01) as determined by Kruskall-Wallis followed by Dunn's multiple comparison. n = 13–50 animals/genotype.

See also Figure S6.

that these genes are acting on developmental morphogenesis rather than directly through a stress-induction pathway. One of the most striking phenotypic differences between the PVD/FLP and IL2 arbors is the ability of the IL2 arbor to retract upon a change in environmental conditions. Future examination of the loss of IL2Q arbors during dauer recovery may provide molecular insight into mechanisms regulating dendritic retraction.

IL2 neurons play roles in dauer maintenance and dauer-specific nictation behavior [4, 33, 34]. *unc-86* and *kpc-1* mutant dauers are defective in both IL2Q arborization and nictation. Furthermore, cell-specific rescue of *kpc-1* restored nictation behavior to wild-type levels. While this evidence is indirect, it is tempting to hypothesize that IL2Q branches have a function in nictation. In the adult, the PVD and FLP neurons are polymodal sensory neurons, serving as both nociceptors and proprioceptors [14, 35, 36]. The morphological similarity between dauer IL2 arbors and PVD/FLP adult arbors may indicate a shared function as polymodal sensory neurons.

We found that *kpc-1* is required for the organization of multidendritic arbors in *C. elegans.* KPC-1 is homologous to furin, an essential mammalian PC [28, 37]. Furin activates semaphorins in vitro and is involved in axon guidance in the developing chick tectum [38, 39], while *Drosophila* Fur1/furin mutants have synaptic target recognition defects [40]. In addition to our discovery of dendrite arborization, we found gross anatomical changes to IL2 axon morphology (Figure S2B); it will therefore be of great interest to examine IL2 synapses with TEM for likely changes in synaptic connectivity in dauer animals and the role of *kpc-1* in these processes.

The substrate(s) of KPC-1 remain elusive. Furin is known to cleave numerous substrates [23]. Based on its similarity with furin, KPC-1 may be necessary for processing TGF-β ligands [28]. However, single mutants of the four TGF-β ligands with predicted furin cleavage sites (*daf-7*, *unc-129*, *dbl-1*, and *tig-2*) did not phenocopy the *kpc-1* mutant IL2 arborization defect (data not shown). The identification of individual substrates responsible for IL2Q arborization is an important but challenging goal. An expansion of our genetic screen, combined with the use of a proteomics approach, may facilitate identification of KPC-1 substrates and understanding of PC biology.

Experimental Procedures

All nematodes were grown under standard conditions [1]. The following transgenic strains were used to image the IL2 neurons and considered wild-type in an N2 Bristol background: PT2519 *myIs13*[P_{klp-6}::GFP + pBX] III; JK2868 *qIs56*[P_{lag-2}::GFP] V [33, 41]; PT2038 *pha-1*; *myEx632* [P_{klp-6}::tdTOMATO + pBX] [42]; PT2506 *ofEx731*[$P_{F28A12.3}$::GFP] [43]. Additional methods are provided in the Supplemental Experimental Procedures.

Supplemental Information

Supplemental Information includes Supplemental Experimental Procedures and six figures and can be found with this article online at http://dx.doi.org/10.1016/j.cub.2013.06.058.

Acknowledgments

We thank the CGC, funded by the NIH Office of Research Infrastructure Programs (P40 OD010440), S. Shaham, T. Lamitina, M. Chalfie, and P. Swoboda for providing strains; Noriko Goldsmith for assistance with confocal microscopy; Natalia Morsci and members of the Barr lab for unpublished data and critical reading of the manuscript; C. Britt Carlson and Michael Klaszky for technical assistance; and David Hall for valuable advice. This work was funded by the USDA (2010-65106-20587) and the New Jersey Commission on Spinal Cord Research (CSCR12FEL004) to N.E.S. and the NIH (5R01DK59418) to MMB.

Received: June 18, 2012
Revised: June 4, 2013
Accepted: June 24, 2013
Published: August 8, 2013

References

1. Brenner, S. (1974). The genetics of *Caenorhabditis elegans*. Genetics *77*, 71–94.
2. Riddle, D.L., and Albert, P.S. (1998). Genetic and environmental regulation of dauer larvae development. In *C. elegans* II, D.L. Riddle, T. Blumenthal, B.J. Meyer, and J.R. Priess, eds. (Plainview: Cold Spring Harbor Laboratory Press), pp. 739–768.
3. Cassada, R.C., and Russell, R.L. (1975). The dauerlarva, a post-embryonic developmental variant of the nematode *Caenorhabditis elegans*. Dev. Biol. *46*, 326–342.
4. Lee, H., Choi, M.K., Lee, D., Kim, H.S., Hwang, H., Kim, H., Park, S., Paik, Y.K., and Lee, J. (2011). Nictation, a dispersal behavior of the nematode *Caenorhabditis elegans*, is regulated by IL2 neurons. Nat. Neurosci. *15*, 107–112.

5. Golden, J.W., and Riddle, D.L. (1984). The *Caenorhabditis elegans* dauer larva: developmental effects of pheromone, food, and temperature. Dev. Biol. *102*, 368–378.
6. Kim, K., and Li, C. (2004). Expression and regulation of an FMRFamide-related neuropeptide gene family in *Caenorhabditis elegans*. J. Comp. Neurol. *475*, 540–550.
7. Peckol, E.L., Troemel, E.R., and Bargmann, C.I. (2001). Sensory experience and sensory activity regulate chemosensory receptor gene expression in *Caenorhabditis elegans*. Proc. Natl. Acad. Sci. USA *98*, 11032–11038.
8. Albert, P.S., and Riddle, D.L. (1983). Developmental alterations in sensory neuroanatomy of the *Caenorhabditis elegans* dauer larva. J. Comp. Neurol. *219*, 461–481.
9. Procko, C., Lu, Y., and Shaham, S. (2011). Glia delimit shape changes of sensory neuron receptive endings in *C. elegans*. Development *138*, 1371–1381.
10. White, J.G., Southgate, E., Thomson, J.N., and Brenner, S. (1986). The structure of the nervous system of the nematode *Caenorhabditis elegans*. Philos. Trans. R. Soc. Lond. B Biol. Sci. *314*, 1–340.
11. Hall, D.H., and Treinin, M. (2011). How does morphology relate to function in sensory arbors? Trends Neurosci. *34*, 443–451.
12. Ward, S., Thomson, N., White, J.G., and Brenner, S. (1975). Electron microscopical reconstruction of the anterior sensory anatomy of the nematode *Caenorhabditis elegans.?*2UU. J. Comp. Neurol. *160*, 313–337.
13. Wang, J., Schwartz, H.T., and Barr, M.M. (2010). Functional specialization of sensory cilia by an RFX transcription factor isoform. Genetics *186*, 1295–1307.
14. Albeg, A., Smith, C.J., Chatzigeorgiou, M., Feitelson, D.G., Hall, D.H., Schafer, W.R., Miller, D.M., 3rd, and Treinin, M. (2011). *C. elegans* multi-dendritic sensory neurons: morphology and function. Mol. Cell. Neurosci. *46*, 308–317.
15. Finney, M., and Ruvkun, G. (1990). The *unc-86* gene product couples cell lineage and cell identity in *C. elegans*. Cell *63*, 895–905.
16. Smith, C.J., Watson, J.D., Spencer, W.C., O'Brien, T., Cha, B., Albeg, A., Treinin, M., and Miller, D.M., 3rd. (2010). Time-lapse imaging and cell-specific expression profiling reveal dynamic branching and molecular determinants of a multi-dendritic nociceptor in *C. elegans*. Dev. Biol. *345*, 18–33.
17. Hamelin, M., Scott, I.M., Way, J.C., and Culotti, J.G. (1992). The *mec-7* β-tubulin gene of *Caenorhabditis elegans* is expressed primarily in the touch receptor neurons. EMBO J. *11*, 2885–2893.
18. Shaham, S., and Bargmann, C.I. (2002). Control of neuronal subtype identity by the *C. elegans* ARID protein CFI-1. Genes Dev. *16*, 972–983.
19. Tsalik, E.L., Niacaris, T., Wenick, A.S., Pau, K., Avery, L., and Hobert, O. (2003). LIM homeobox gene-dependent expression of biogenic amine receptors in restricted regions of the *C. elegans* nervous system. Dev. Biol. *263*, 81–102.
20. Way, J.C., and Chalfie, M. (1988). *mec-3*, a homeobox-containing gene that specifies differentiation of the touch receptor neurons in *C. elegans*. Cell *54*, 5–16.
21. Perkins, L.A., Hedgecock, E.M., Thomson, J.N., and Culotti, J.G. (1986). Mutant sensory cilia in the nematode *Caenorhabditis elegans*. Dev. Biol. *117*, 456–487.
22. Swoboda, P., Adler, H.T., and Thomas, J.H. (2000). The RFX-type transcription factor DAF-19 regulates sensory neuron cilium formation in *C. elegans*. Mol. Cell *5*, 411–421.
23. Artenstein, A.W., and Opal, S.M. (2011). Proprotein convertases in health and disease. N. Engl. J. Med. *365*, 2507–2518.
24. Seidah, N.G., and Prat, A. (2012). The biology and therapeutic targeting of the proprotein convertases. Nat. Rev. Drug Discov. *11*, 367–383.
25. Zhou, A., Martin, S., Lipkind, G., LaMendola, J., and Steiner, D.F. (1998). Regulatory roles of the P domain of the subtilisin-like prohormone convertases. J. Biol. Chem. *273*, 11107–11114.
26. Seidah, N.G. (2011). The proprotein convertases, 20 years later. Methods Mol. Biol. *768*, 23–57.
27. Henrich, S., Cameron, A., Bourenkov, G.P., Kiefersauer, R., Huber, R., Lindberg, I., Bode, W., and Than, M.E. (2003). The crystal structure of the proprotein processing proteinase furin explains its stringent specificity. Nat. Struct. Biol. *10*, 520–526.
28. Thacker, C., and Rose, A.M. (2000). A look at the *Caenorhabditis elegans* Kex2/Subtilisin-like proprotein convertase family. Bioessays *22*, 545–553.
29. Liu, T., Kim, K., Li, C., and Barr, M.M. (2007). FMRFamide-like neuropeptides and mechanosensory touch receptor neurons regulate male sexual turning behavior in *Caenorhabditis elegans*. J. Neurosci. *27*, 7174–7182.
30. Kulkarni, V.A., and Firestein, B.L. (2012). The dendritic tree and brain disorders. Mol. Cell. Neurosci. *50*, 10–20.
31. Vyas, A., Mitra, R., Shankaranarayana Rao, B.S., and Chattarji, S. (2002). Chronic stress induces contrasting patterns of dendritic remodeling in hippocampal and amygdaloid neurons. J. Neurosci. *22*, 6810–6818.
32. Miller, M.M., and McEwen, B.S. (2006). Establishing an agenda for translational research on PTSD. Ann. N Y Acad. Sci. *1071*, 294–312.
33. Ouellet, J., Li, S., and Roy, R. (2008). Notch signalling is required for both dauer maintenance and recovery in *C. elegans*. Development *135*, 2583–2592.
34. Lewis, J.A., and Hodgkin, J.A. (1977). Specific neuroanatomical changes in chemosensory mutants of the nematode *Caenorhabditis elegans*. J. Comp. Neurol. *172*, 489–510.
35. Chatzigeorgiou, M., Yoo, S., Watson, J.D., Lee, W.H., Spencer, W.C., Kindt, K.S., Hwang, S.W., Miller, D.M., 3rd, Treinin, M., Driscoll, M., and Schafer, W.R. (2010). Specific roles for DEG/ENaC and TRP channels in touch and thermosensation in *C. elegans* nociceptors. Nat. Neurosci. *13*, 861–868.
36. Liu, S., Schulze, E., and Baumeister, R. (2012). Temperature- and touch-sensitive neurons couple CNG and TRPV channel activities to control heat avoidance in *Caenorhabditis elegans*. PLoS ONE *7*, e32360.
37. Roebroek, A.J., Umans, L., Pauli, I.G., Robertson, E.J., van Leuven, F., Van de Ven, W.J., and Constam, D.B. (1998). Failure of ventral closure and axial rotation in embryos lacking the proprotein convertase Furin. Development *125*, 4863–4876.
38. Tassew, N.G., Charish, J., Seidah, N.G., and Monnier, P.P. (2012). SKI-1 and Furin generate multiple RGMa fragments that regulate axonal growth. Dev. Cell *22*, 391–402.
39. Adams, R.H., Lohrum, M., Klostermann, A., Betz, H., and Püschel, A.W. (1997). The chemorepulsive activity of secreted semaphorins is regulated by furin-dependent proteolytic processing. EMBO J. *16*, 6077–6086.
40. Kurusu, M., Cording, A., Taniguchi, M., Menon, K., Suzuki, E., and Zinn, K. (2008). A screen of cell-surface molecules identifies leucine-rich repeat proteins as key mediators of synaptic target selection. Neuron *59*, 972–985.
41. Blelloch, R., Anna-Arriola, S.S., Gao, D., Li, Y., Hodgkin, J., and Kimble, J. (1999). The *gon-1* gene is required for gonadal morphogenesis in *Caenorhabditis elegans*. Dev. Biol. *216*, 382–393.
42. Peden, E.M., and Barr, M.M. (2005). The KLP-6 kinesin is required for male mating behaviors and Polycystin localization in *Caenorhabditis elegans*. Curr. Biol. *15*, 394–404.
43. Phirke, P., Efimenko, E., Mohan, S., Burghoorn, J., Crona, F., Bakhoum, M.W., Trieb, M., Schuske, K., Jorgensen, E.M., Piasecki, B.P., et al. (2011). Transcriptional profiling of *C. elegans* DAF-19 uncovers a ciliary base-associated protein and a CDK/CCRK/LF2p-related kinase required for intraflagellar transport. Dev. Biol. *357*, 235–247.